



REVIEW ON FINITE ELEMENT ANALYSIS OF SHEET METAL STRETCH FLANGING PROCESS

Yogesh Dewang¹, M. S. Hora² and S. K. Panthi³

¹Department of Mechanical Engineering, Maulana Azad National Institute of Technology, Bhopal, India

²Department of Civil Engineering, Maulana Azad National Institute of Technology, Bhopal, India

³Computer Simulation and Design Centre, Advanced Materials Processes and Research Institute, Bhopal, India

E-Mail: yogesh_dewang@yahoo.co.in

ABSTRACT

This paper presents a review of finite element analysis of stretch flanging process and its finite element simulation, finite element formulation and finite element method (FEM) based parametric studies and their results. Stretch flanging process is secondary sheet metal forming process which is widely used in conjunction with other sheet metal forming process in sheet metal forming industry. It is used for making of automotive components and complex panels. In past researchers had worked on the area of finite element analysis of stretch flanging process in terms of development of FEM based computer programs and by using different commercial FEM software packages. It is observed that majority of finite element simulation for stretch flanging processes have employed explicit dynamic FEM approach. It is also found from FEM based parametric studies that geometrical parameters have greater influence upon the formability of stretch flanging process as compared to material parameters. Besides this, it is also observed that for manufacturing of stretch flange parts and components ferrous alloys were used in past, whereas aluminum alloys being used commonly in present scenario for obtaining corrosion free and lightweight with increased strength parts. Hence, it is found that analysis based on finite element method is a powerful, accurate and efficient technique for better designing of stretch flanging process.

Keywords: finite element analysis, stretch flanging, simulation, strain.

1. INTRODUCTION

Flanging is a sheet metal bending operation which is applied in automobile industry in which sheet is bent usually to 90 degree for providing a smooth rounded edge, higher rigidity or strength to the edge of sheet-metal parts. Flanging is similar to bending of sheet metal except that during flanging, the metal bent down is short compared with the overall part size. Most forming operations in automobile production have to undergo with the formation of flanges. Many straight bending operations are used in making flanges. These involve forming under combined compressive and tensile conditions using a punch and die to raise closed rims on pierced holes. Flanging is also used for making hidden joints and assembly of automobile parts.

Flanges are mainly of three types i.e. straight flange, shrink flanges and stretch flanges as shown in Figure-1. In straight flanges the sheet is bent along a straight line usually to 90 degree resulting in localized plane strain deformation of the sheet. The remaining types of flanges i.e. stretch flange and shrink flange are contoured flanges. In case of contoured flanges, the sheet is formed along a curved line and due to the curvature of bending line the deformation is not plane strain but three dimensional. A shrink flange has a convex curvature. In forming a shrink flange, the metal used to form the flange must be reduced in length. This relationship is easily seen in the flanging of a circular cake pan in which the diameter of the finished flange is less than the diameter of the disk from which it was formed. A stretch flange has a concave curvature. It is called a stretch flange because the material forming the flange must be stretched. This stretching is easily seen in forming of a flange for a hole. The metal

used in forming the flange must be elongated. There is another type of flange which is a combination of all three types of flanges and it consists of three different portions of bend which represents straight, stretch and shrink flanges as shown in Figure-1. It is an example of complex panels which is being used in industrial practice. (Semiatin S.L., 2006). The objective of the present paper is to review the sheet metal stretch flanging process in the area of its finite element analysis.

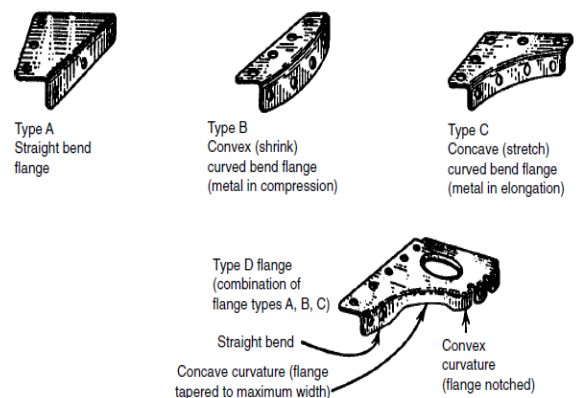


Figure-1. Different types of flanges (Semiatin S.L., 2006).

2. OVERVIEW OF STRETCH FLANGING PROCESS

Stretch flanging process is one of the common sheet metal forming operations. On the basis of product obtained after flanging operation, stretch flanging can be classified as stretch flanging without hole and stretch flanging with hole. Figure-2 shows tooling-set for non-



axisymmetric stretch flanging process, in which the sheet sample is situated between a fixed die and a blank-holder. A blank-holding force is applied over the blank-holder to keep the sheet samples to remain fixed between die and blank-holder. A side-ward punch is situated at an appropriate clearance with die for bending the sheet over the die for making stretch flange without hole. The door panels of the cars are one of the examples of stretch flanging without hole which are commercially used as shown in Figure-3.

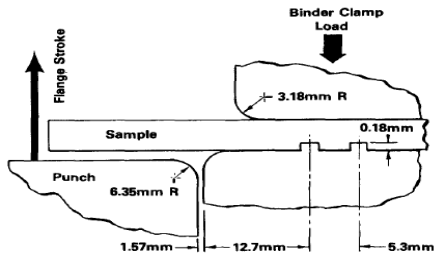


Figure-2. Tool-set for stretch flanging without hole (Dudra S., Shah S., 1988).

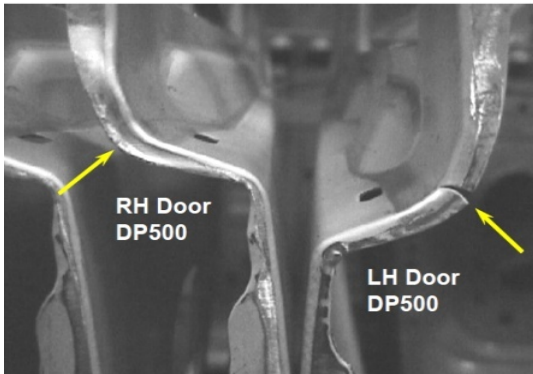


Figure-3. Stretch flange without hole.

In contrast to this, Figure-3 shows the schematic diagram of the tooling-set of stretch flanging with hole, also known as hole-flanging process. The tool-setup for stretch flanging with hole is meant for obtaining axisymmetric products. The tooling setup consists of sheet samples with pre-cut hole in the center, which is held between die and blank-holder. A blank-holding force is applied over the blank-holder to restrain the sheet sample for flanging operation. A punch is situated in the center of the axisymmetric tooling-set up for making stretch flange with hole as shown in Figure-3. Due to the flanging stroke of punch the pre-cut hole sample is expanded into a lip form in the vertical direction, and such type of product is obtained after stretch flanging as shown in Figure-5.

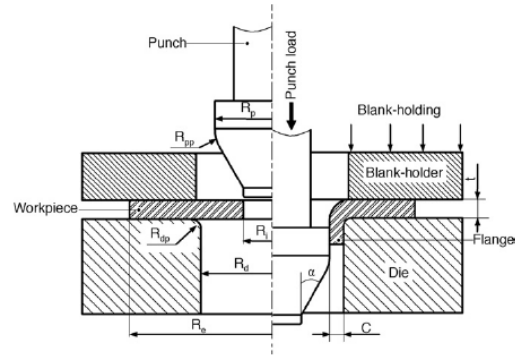


Figure-4. Tool-setup for stretch flanging with hole (Kacem Ahmed et al, 2011).

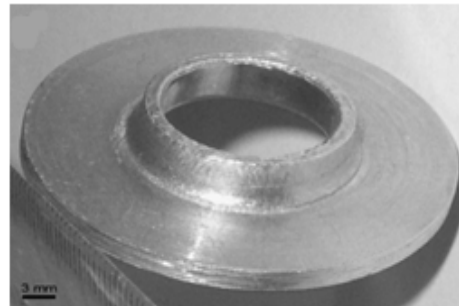


Figure-5. Stretch flange with hole (Krichen A. et al, 2011).

Stretch flanging and hole flanging process involve the two-tension stress state (from the uniaxial-tension state to the plane-strain state) where stretching is the major deformation. In the tension-compression state (OB-OC, OA-OF), the tension as the major deformation infers that the thickness is reduced as shown in Figure-6. If ϵ_{maj} is the tensile principal strain, then the compression strain can be expressed as (Hu W., Wang Z.R., 2002).

$$\epsilon_{min} = -\frac{R}{1+R} \epsilon_{maj} - \frac{\sqrt{1+2R}}{1+R} (\epsilon_1^2 - \epsilon_{maj}^2)^{\frac{1}{2}} \quad (1)$$

The three principal strain distribution with the R-value changing are given as

$$\begin{aligned} R \uparrow, \epsilon_{11B}(R_1) (\epsilon_{tB}(R_1)) &> \epsilon_{11B}(R_0) (\epsilon_{tB}(R_0)), \\ |\epsilon_{22C}(R_1)| &< |\epsilon_{22C}(R_0)|, \epsilon_{tC}(R_1) = \epsilon_{tC}(R_0) = 0, \\ R \rightarrow \infty, \epsilon_{22} &\rightarrow -\epsilon_{11}, \epsilon_t \rightarrow 0, \\ R \downarrow, \epsilon_{11B}(R_1) (\epsilon_{tB}(R_1)) &< \epsilon_{11B}(R_0) (\epsilon_{tB}(R_0)), \\ |\epsilon_{22C}(R_1)| &> |\epsilon_{22C}(R_0)|, \epsilon_{tC}(R_1) = \epsilon_{tC}(R_0) = 0, \\ R \rightarrow 0, \epsilon_t &\rightarrow -\epsilon_{11}, \epsilon_{22} \rightarrow 0, \text{ (in bi-tension stress area),} \end{aligned}$$

$$\epsilon_{11} \geq 0, \epsilon_{22} \leq 0, \tau_t \leq 0 \quad (2)$$

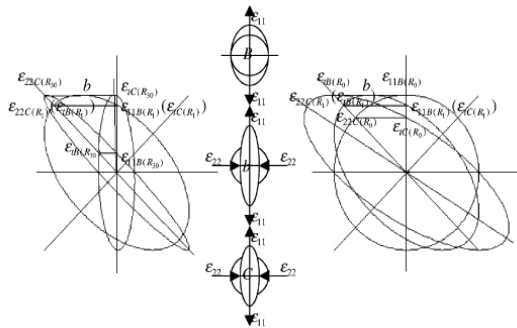


Figure-6. Strain change with R-value (Hu W., Wang Z.R., 2002).

Where $\epsilon_{11C}(R_j), \epsilon_{11B}(R_j), \epsilon_{11A}(R_j)$ ($j=0, 1, 30$) are the absolute principal strains and the thickness strains on the points C and B respectively with different R-values ($R=0, R=1, R=30$). This means with increase of R-values, the values of ϵ_{11} (or $\epsilon_{11(22)}$) and thinning near to the plane-strain state (point B or A) decreases, and the absolute values of two principal strains near to the plane-strain state (points C and F) slightly increases. When the R-value approaches zero, the thinning becomes most serious as shown in Figure-7.

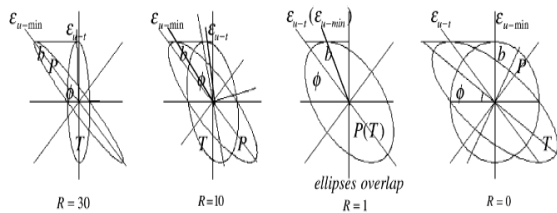


Figure-7. Thinning behavior based on anisotropic property (Hu W., Wang Z.R., 2002).

Between the uniaxial-tension and plane strain state (points B and A), the primary forming failure are due to thinning and splitting. Near the plane-strain state (points C and F), the main forming failure is fracture in stretch flanging. In order to reduce these problems, a greater R-value should be selected. The $R \gg 1$ should be selected for stretch flanging process to avoid fracture. (Hu W., Wang Z.R., 2002)

3. THEORETICAL DESCRIPTION

3.1. FEM simulation

FEM simulation is a means of predicting the behavior of various complex objects or systems that are often connected, without having to rely on physically existing models, prototypes or measurements. It involves numerically dividing the system being analyzed into a, often, very large number of small (finite) volumes, calculating the physical states (stresses, field strengths, temperatures, etc.) of each individual cell and using an iterative process to approximate the neighbouring cells

until a physically practical solution is obtained for the overall system. Finite element method can be used to examine problems and to find a potential solution in various physical conditions. Finite element simulation is one of the powerful tools to analyze any sheet metal forming processes. It reduces the number of tryouts and save labour and time, which usually occurs in performing experiments. In nutshell benefits of FEM include increased accuracy, enhanced design and better insight into critical design parameters, virtual prototyping, fewer hardware prototypes, a faster and less expensive design cycle, increased productivity, and increased revenue.

3.2. Finite element formulation

Finite element method (FEM) is a numerical method for solving a differential or integral equation. It has been widely applied to a number of physical problems where the governing differential equations are available. The method essentially consists of assuming the piecewise continuous function for the solution and obtaining the parameters of the functions in a manner that reduces the error in the solution. In finite element method for obtaining solution of problem the governing equations are formulated by using partial differential equations in their nascent form. Then these governing equations are converted into weak form such that domain integration can be utilized to satisfy the governing equations in an average sense.

A functional Π is set up for the system, which describes the energy or energy rate and implies that the solution can be found by minimization. For a generic functional, this is written as

$$\frac{\delta \Pi}{\delta u} = \frac{\delta}{\delta u} \left(\int f(x_i, u_i) dV \right) = \frac{\delta}{\delta u} \left(\sum_j f(x_i, u_i) \Delta V_j \right) = 0 \quad (3)$$

where the functional is a function of the coordinates x_i and the primary variable u_i being e.g. displacements or velocities. The domain integration is approximated by a summation over a finite number of elements discretizing the domain. Figure-8 illustrates a three dimensional domain discretized by hexahedral elements with eight nodes. The variables are defined and solved in the nodal points, and evaluation of variables in the domain is performed by interpolation in each element. Shared nodes give rise to an assembly of elements into a global system of equations of the form;

$$Ku = f \quad (4)$$

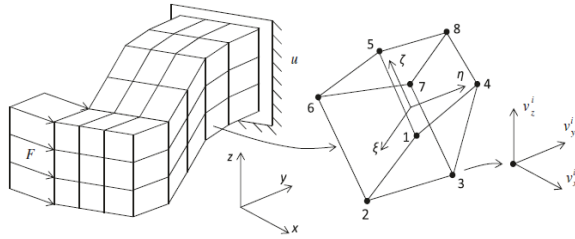


Figure-8. Illustration of three-dimensional finite element model composed of isoparametric, hexahedral elements with eight nodes.

Each node has three degrees of freedom for representation of vector fields and one degree of freedom for representation of scalar fields.

where K is the stiffness matrix, u is the primary variable and f is the applied load, e.g. stemming from applied tractions F on a surface S_F in Figure-8. The system of equations (4) is furthermore subject to essential boundary conditions, e.g. prescribed displacements or velocities u along a surface S_U . (Nielsen C.V. *et al.*, 2013) In context of finite element analysis of stretch flanging process an explicit dynamic finite element approach was employed (Yeh F.H. *et al.*, 2007). They have utilized this explicit dynamic FEM formulation which is based on virtual work governing equation which involves internal force, body force, contact force and momentum which can be expressed as following (Yeh F.H. *et al.*, 2007):

$$\int \rho \dot{x} \delta x \, dV + \int \sigma \delta \epsilon \, dV - \int \rho b \delta x \, dV - \int f \delta x \, dS = 0 \quad (5)$$

Where \ddot{x} is the acceleration, σ the Cauchy stress, ϵ the strain, ρ the mass density, b the body force density and f the surface traction force. After the finite element discretion, Equation (5) will be described in a matrix form as

$$M \ddot{u} = F_t^1 + F_t^2 + F_t^3 \quad (6)$$

and

$$M = \sum \int \rho N^T N \, dV$$

$$F_t^1 = \sum \int B^T \sigma \, dV$$

$$F_t^2 = \sum \int \rho N^T b \, dV$$

$$F_t^3 = \sum \int N^T f \, dS$$

Where M is the mass matrix, F_t^1 , F_t^2 and F_t^3 are the stress load, body force load, and surface force load at time t , respectively. N is the shape function. The solution for

time $t + \Delta t$ can be obtained by solving the acceleration \ddot{u} in Equation (6) firstly. Then, the central difference method was used to calculate velocity and displacement as follows:

$$\ddot{u}_{t+\Delta t} = M^{-1}(-1) (F_{t+\Delta t}^1 + F_{t+\Delta t}^2 + F_{t+\Delta t}^3) \quad (7)$$

$$v_{t+\frac{\Delta t}{2}} = v_{t-\frac{\Delta t}{2}} + \ddot{u}_t \Delta t \quad (8)$$

$$u_{t+\Delta t} = u_t + v_{t+\frac{\Delta t}{2}} \Delta t \quad (9)$$

Where $\frac{\Delta t_{t+\Delta t}}{2} = 0.5 (\Delta t_t + \Delta t_{t+\Delta t})$, v and u are the nodal velocity and displacement.

It is clear that the time increment Δt in the central difference method should be small than a critical time increment Δt_{crit} in order to guarantee the convergence in the solution procedure, and the critical time increment Δt_{crit} for the shell element in the explicit dynamic scheme is decided from Equation (10):

$$\Delta t_{crit} = \frac{L_s}{\sqrt{\frac{E}{\rho(1-\nu^2)}}} \quad (10)$$

where L_s is the characteristic length that is calculated from element area divides the longest side in the element. E and ν are the Young's modulus and Poisson's ratio, respectively. As each element has its critical time increment, the critical time increment in a deformation stage will be determined from the minimum value in the whole system. i.e.

$$\Delta t_{\Delta t} = \alpha \min \{ \Delta t_1, \Delta t_2, \dots, \Delta t_n \} \quad (11)$$

where n denotes the element number. Δt_i is the critical time increment for element i , and α is a safety parameter which usual sets to be 0.9 in the simulation. It is clear that the time increment in Equation (10) is proportional to the square root of the mass density. Therefore it is found that explicit dynamic FEM formulation has got the advantage of maintaining accuracy with reduced execution time.

4. FINITE ELEMENT ANALYSIS

Although, finite element analysis of stretch flanging process is a difficult task, but due to rapid development and growth in numerical and computational facilities available in market as commercial packages based on FEM enables the successful simulation of stretch flanging process both at industrial and lab-scale levels. In stretch flanging, finite element simulation were carried out by researchers to get insight of the process. In past various types of numerical solution i.e., based on computer program and commercial FE software packages were used to study the stretch flanging process which are described under following sections.



4.1. Materials and constitutive material models

In past researchers had employed different materials for conducting finite element analysis through computer based FEM program as well as through commercial FEM software packages. In view of finite element simulation of stretch flanging process selection of material and as well as proper material model is a primary and major task. For conducting finite element analysis of stretch flanging process, various types of ferrous alloys

such as AKDQ steel, cold rolled steel and other sheet metal alloys were commonly used in the past two decades. In past decade up to present scenario stretch flanges are now made by using AHSS and Al-Mg alloys such as AA 5182 and AA5752. Generally, for FEM simulation in stretch flanging material is considered as elasto-plastic. Table-1 shows the materials used by researchers in the past for making stretch flanges. It also present the materials properties such as Modulus of

Table-1. Materials and mechanical properties of materials for stretch flange forming.

Author	Year	Material	Material properties							
			Modulus of elasticity E (GPa)	Poisson s ratio (μ)	Sheet thickness (t) (mm)	Yield Strength (σ_y) (MPa)	Ultimate tensile strength σ_{ut} (MPa)	Elongation Δl (%)	Reference stress (K) (MPa)	Strain hardening exponent (n)
Wang N.M. <i>et al</i>	1984	AKDQ steel	206.8	n.a.	n.a.	184	316	37.9	538	0.21
		HSLA Steel	206.8	n.a.	n.a.	436	510	22	816	0.16
		2036-T4	68.9	n.a.	n.a.	209	359	23	665	0.22
Dudra S. and Shah S.	1988	1008 AK steel	210	n.a.	0.69	168.2	293	39	503.1	0.23
Wang C.T. <i>et al.</i>	1995	High strength steel	206.8	0.3	0.91	n.a.	289	n.a.	603.8	0.143
Hu P. <i>et al.</i>	2003	09CuP	207	0.3	8	n.a.	n.a.	n.a.	587.9	0.143
Feng X. <i>et al.</i>	2004	Sheet metal	206	0.3	1	167	n.a.	n.a.	565.32	0.2589
Chen Z. <i>et al.</i>	2005	AA 5182	71.71	0.33	1.6	117.34	n.a.	n.a.	n.a.	n.a.
		AA 5754	71.71	0.33	1.6	102.78	n.a.	n.a.	n.a.	n.a.
Butcher <i>et al.</i>	2006	AA 5182	71.71	0.33	1.6	117.34	n.a.	n.a.	n.a.	n.a.
Li D. <i>et al.</i>	2007	Sheet metal	n.a.	n.a.	1	n.a.	n.a.	n.a.	538	0.216
Bao Y.D. and Huh H.	2007	Sheet metal	n.a.	n.a.	1	n.a.	n.a.	n.a.	549.03	0.22
Yeh F.H. <i>et al</i>	2007	SPCEN-SD (DDQ)	210	0.3	1	160	n.a.	n.a.	516.54	0.232

Table-2. Constitutive material models used in stretch flanging FEM analysis.

S. No.	Author	Year	Constitutive relationship
1.	Wang, N.M. <i>et al</i>	1984	$\varepsilon = \frac{\sigma}{E} + \frac{\sigma^n}{K}$
2.	Asnafi N.	1991	$\sigma_y = K (\varepsilon^E + \varepsilon^P)^n$
3.	Feng X.	2004	$\sigma = 565.32(0.007117 + \varepsilon_p)^{0.2589}$
4.	Yeh F.H. <i>et al</i>	2007	$\bar{\sigma} = 516.54 (0.00639 + \bar{\varepsilon}_p)^{0.232}$
5.	Dayong <i>et al.</i>	2007	$\bar{\sigma} = K \bar{\varepsilon}^n$
6.	Bao Y.D. and Huh H.	2007	$\bar{\sigma} = 549.03 (0.0013 + \bar{\varepsilon}_p)^{0.22}$



Elasticity, poisson's ratio, yield strength, ultimate tensile strength, strain hardening exponent, anisotropy parameter, etc. which are used as inputs for conducting FEM simulation. On the other hand, another aspect of numerical simulation related to material is constitutive material model which is being used in finite element simulation of stretch flanging process. Constitutive material model signifies the stress-strain relationship after conducting various types of tests on material for obtaining constitutive relationship which shows the behavior of material in real conditions.

4.2. Geometries of stretch flange

Different types of geometries were considered by researchers in the past for FEM analysis of stretch flanging process. One of the type of geometry is simple stretch flange or non-axisymmetric stretch flange consists of bending the sheet along die in a side-ward direction without making any hole as a shown in Figure-9.

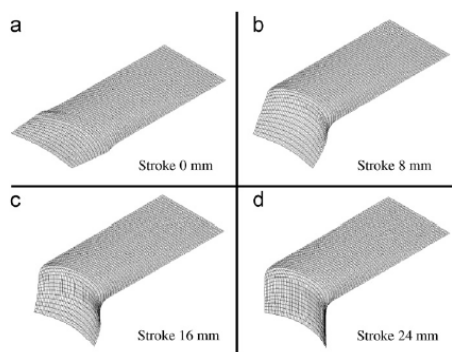


Figure-9. Simple stretch flange (Yeh F.H. *et al.*, 2007).

Finite element analysis of simple stretch flange was carried out by many researchers in the past (Worswick M.J., Finn M.J., 2000; Yeh F.H. *et al.*, 2007). Another type of stretch flange is axisymmetric stretch flange in which the sheet sample is taken with a pre-cut hole in center and is bent with the help of axisymmetric punch over the die to obtain the extended lip height as shown in Figure-10.

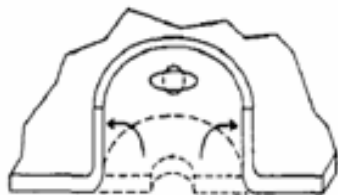


Figure-10. Stretch flange with hole (Wang C.T. *et al.*, 1995).

In these type of flanges finite element analysis were carried out by many researchers in the past (Demeri M.Y. and Tang S.C., 1991; Wang. C.T. *et al.*, 1995; Asnafi N., 1999; Huang M.Y., 2007; Huang M.Y., 2007). Stretch flange are also made by "V" shaped sheet metal blanks.

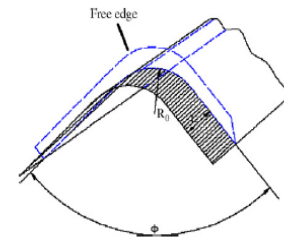


Figure-11. V-shaped stretch flanges (Dayong L. *et al.*, 2007).

In this type of stretch flange the sheet is bent into the form of "V" as shown in Figure-11. FEM analysis of "V" shaped stretch flange was done by various researchers (Wang N.M *et al.*, 1984; Dudra S. and Shah S., 1988; Dayong Li *et al.*, 2007). Finite element analysis of stretch curved flanging was carried in the past. For making this type of stretch flange, two movements are considered during flanging. First the binder moves until it clamps the sheet on the die. This movement could result in the bent sheet as shown in Figure-12(a). After that, the punch moves upwards to flange the bent sheet with pressure applied on the binder to clamp the sheet. Finally, the final deformed sheet is obtained as shown in Figure-12(b) (Feng X. *et al.*, 2004). Another type of stretch flange is z-flange as shown in Figure-13. Numerical simulation of z-stretch flange is also carried out in the past by researchers. (Worswick M.J., Finn M.J., 2000; Chen Z. *et al.*, 2005; Butcher C. *et al.*, 2006; Simha C.H.M. *et al.*, 2008; VafaeesefatA, Khanahmadlu)

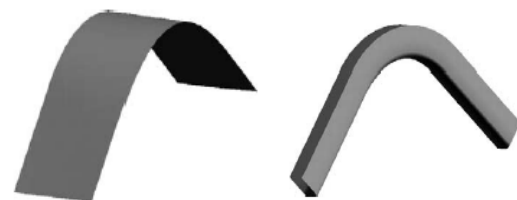


Figure-12(a). Stretch curved flange initial position
(b) stretch curved flange after bent position (Feng X. *et al.*, 2007).

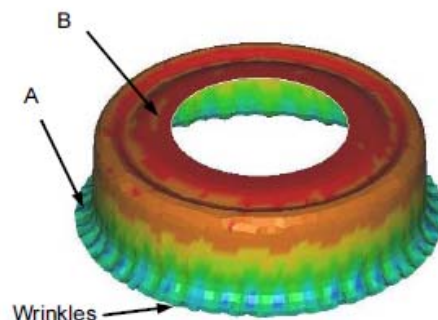


Figure-13. Stretch z-flange with drawbead (Vafaeesat A., Khanahmadlu M., 2011).



4.3 Modeling and simulation

In stretch flanging of V-shaped metal blanks a general purpose finite element computer program was developed on the basis of a total lagrangian plane stress formulation for obtaining a numerical solution of the in-plane stretching model. They have considered the material as elasto-plastic for FEM simulation. The FEM formulations utilized satisfy Hill's normally anisotropic, rate insensitive yield theory. They also incorporated the effect of strain hardening by using Ramberg-Osgood stress-strain law. For simulation of stretch flanging process, they have utilized constant stress (strain) triangular elements for sheet material in computer program (Wang N.M. *et al*, 1984). In stretch flanging of 1008 AK steel finite element method program was employed for prediction of strain in case of non-axisymmetric stretch flange (Dudra S. and Shah S., 1988). Figure-14 shows the finite element mesh for finite element analysis of stretch flanging process.

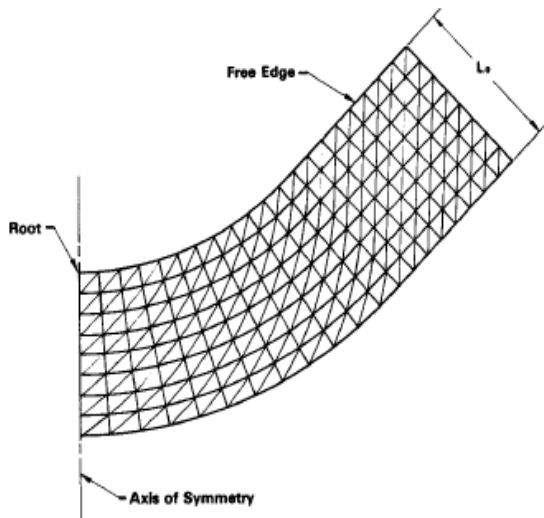


Figure-14. Finite element mesh used in FEM analysis (Dudra S. and Shah S., 1988).

In stretch flanging of 1 and 1.6 mm thick AA 2024-O and AA 6061-O by fluid forming (Asnafi N., 1999) used a FEM code LS-DYNA3D to simulate the process. In finite element simulations, he considered both sheets to be elasto-plastic material. He has considered the forming limit curve of material AA-2024-O to predict the onset of failure in stretch flanging. Finite element simulation of stretch flange forming was carried out by (Worswick M.J. and Finn M.J., 2000) using explicit dynamic finite element approach utilizing various quadratic and non-quadratic yield criteria. They have used four noded shell elements for tools while blank was modeled using four noded quadrilateral, Belytschko-Lin-Tsay shell elements. Different cases of circular stretch flange, square cut-out stretch flange, square cut-out stretch flange and a model of an automotive inner panel are simulated for prediction of strain as shown in Figure-15(a-d), respectively.

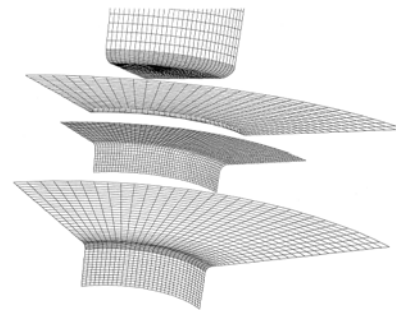
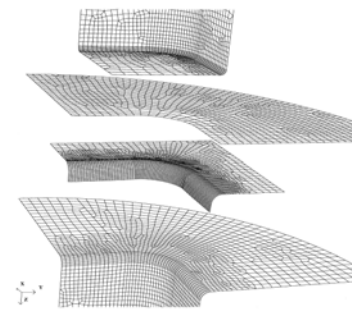
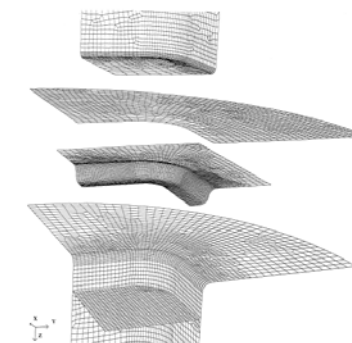


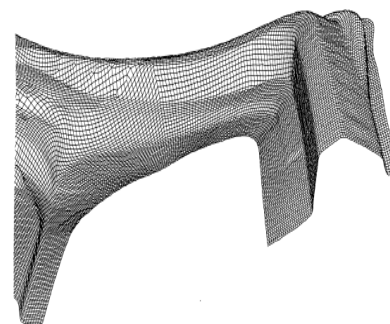
Figure-15(a). FEM model of circular stretch flange with mesh.



(b) FEM model of square cut-out stretch flange with mesh.



(c) FEM model of square cut-out stretch z-flange with mesh.



(d) FEM model of automotive inner panel showing stretch flange corner feature (Worswick M.J. and Finn M.J., 2000).

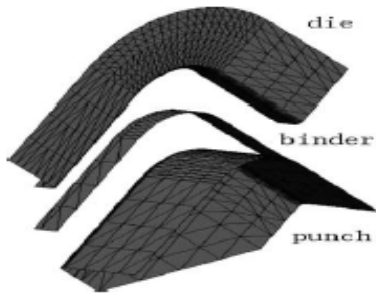


Figure-16. FEM model of stretch curved flanging (Feng X. *et al*, 2007).

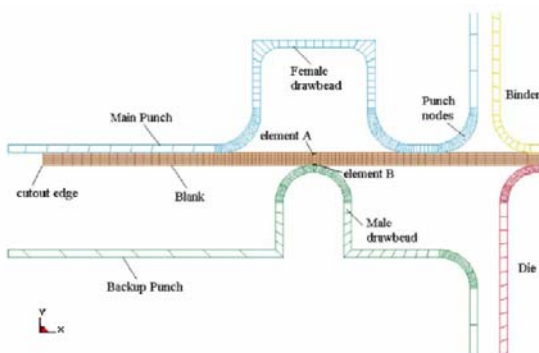


Figure-17. Axisymmetric finite element mesh used to model stretch flange forming operation (Chen Z. *et al*, 2005).

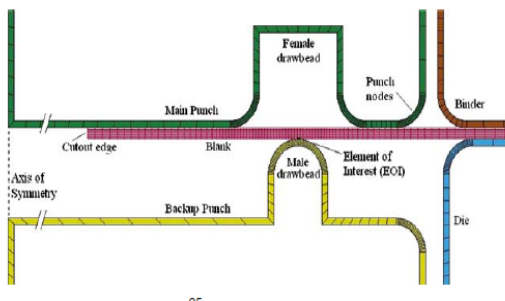


Figure-18. FE mesh of blank and tooling (Butcher C. *et al*, 2006).

A static implicit code Autoform and explicit FEM code LS-DYNA 3D was used for finite element simulation of stretch curved flanging of sheet metal. Figure-16 shows the FEM model for stretch curved flanging by (Feng X. *et al*, 2004). In another FEM analysis of stretch flange forming of AA 5182 and AA 5754 sheets, a multi-scale finite element (FE) damage percolation model was employed for finite element simulation as shown in Figure-17. They have used GTN model and predicted the formability of stretch flange based upon the onset of catastrophic failure triggered by profuse void coalescence within the measured second-phase particle field (Chen Z. *et al*, 2005). A three-dimensional axisymmetric finite element model was developed to simulate the stretch

flange forming process of AA 5182 sheet as shown in Figure-18. They have employed GTN and STN models into explicit LS-DYNA finite element code using the “elastic predictor-normal corrector” method for finite element simulation (Butcher C. *et al*, 2006). An elastic-plastic large deformation FEM program was developed on Mindlin shell element model for simulation of stretch flanging of V-shaped sheet metal. Figure-19 (a-b) shows the finite element model and sheet metal blank after meshing respectively (Li D. *et al*, 2007).

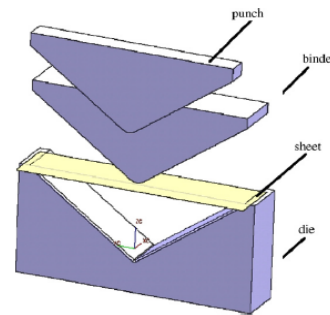
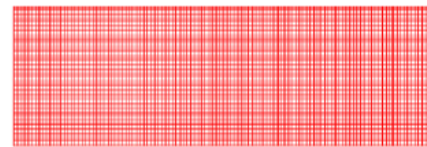


Figure-19(a). FEM model for “V” shaped stretch flanging.



(b) Finite element mesh of sheet metal blank (Li D. *et al*, 2007).

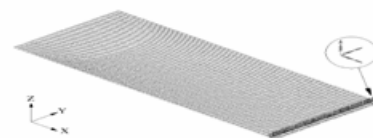


Figure-20. Finite element meshes (Yeh F.H. *et al*, 2007).

An explicit dynamic finite element approach was utilized to simulate stretch flange forming process. A three dimensional finite element model is generated using shell elements in a quarter part. This generated finite element model involves 3000 elements and 3111 nodes after meshing as shown in Figure-20 (Yeh F.H. *et al*, 2007). The incremental updated Lagrangian elasto-plastic finite element method (FEM) was employed to analyze the stretch flange of circular plates with a pre-determined smaller hole at the centre of sheet metal. Four-node quadrilateral element was adopted in one integration point for the stabilization matrix, which is efficient for axisymmetric stretch flange forming (Huang Y.M., 2007). In another attempt of stretch flange forming of 1.6 mm thick AA 5754 and 1 mm thick AA 5182 finite element simulation was carried out using LS-DYNA finite element



software. They have discretized the blank first with Belytschko plane stress elements and then modeled the blank with eight noded solid elements in order to assess the effect of plane stress elements as shown in Figure-21. They found on comparison between computations of plane stress elements that plane stress approximation was not valid (Simha C.H.M. *et al.*, 2008).

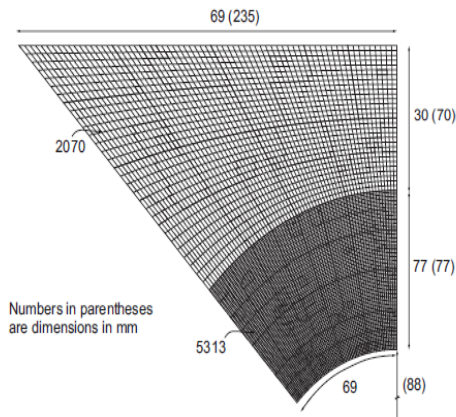


Figure-21. Mesh used in the shell element computations (Simha C.H.M. *et al.*, 2008).

Finite element analysis of stretch flanging process by rubber forming using AA 2024-O was carried out by using commercially available FEA software Pamstamp. Figure-22 shows the finite element model for stretch flanging with rubber forming (Yingwei C.L.L., Shanliang L., 2010). In finite element simulation of sheet metal z-stretch flange an explicit dynamic finite element code LS-DYNA was employed. Figure-23 shows the Figure for finite element model for z-stretch flange. Four different types of shell elements were used to obtain accurate results. The shell elements used by them were shown in Table-3 with average deviations and computational time needed. Firstly, they used Belytschko-Tsay (B-T) element, which was based on a perfectly flat geometry. Secondly, they used the shell element named Belytschko-Leviathan (B-L) element which has a physical hourglass control and therefore does not need any user defined hourglass coefficient. Thirdly, they used Belytschko-Wong-Chiang element (B-W-C) which was a simple and computationally inexpensive modification necessary in the B-T shell to include warping and stiffness. Finally they used the H-L shell element which assumes non-planar geometry and gives good results on the twisted beam, but is relatively expensive. Table-3 shows the summary CPU time used for simulation results. They found that FE simulation with B-T shell elements can slightly better predict the flange forming process in a shorter time (Vafaeseefat A. and Khanahmadlu M., 2011).

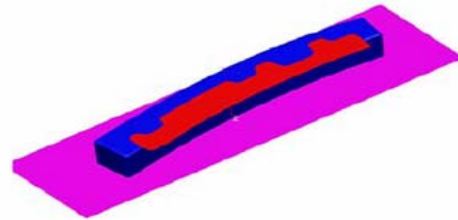


Figure-22. FEM model for stretch flanging with rubber forming (Yingwei C.L.L., Shanliang L., 2010).

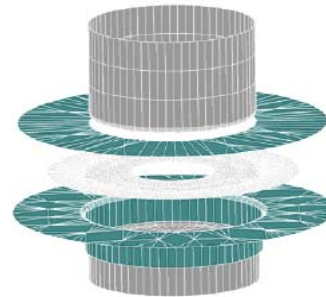


Figure-23. FEM model used for stretch-z-flanging (Vafaeseefat A., Khanahmadlu M., 2011).

Table-3. Comparison of computational time for different shell elements types (Vafaeseefat A., Khanahmadlu M., 2011).

Element type	B-L	B-T	B-W-C	H-L
Average deviations	1.441535	1.414278	1.371939	2.056484
CPU time (sec)	1851	1707	1720	2456

Finite element simulation of stretch flanging process was carried in order to analyze the deformation behavior of stretch flange of cold rolled steel and AKDQ steel by using ABAQUS FEM code. Figure-24(a) shows the finite element mesh of the sheet metal with 4-noded doubly curved thin shell element with reduced integration with finite strain (S4R). Figure-24(b) shows the finite element model of stretch flanging process by using axisymmetric die (Dewang Y. *et al.*, 2014).

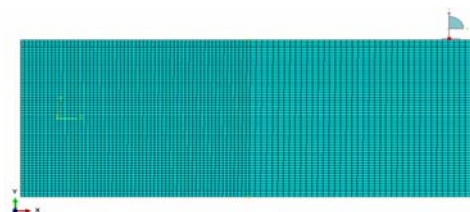
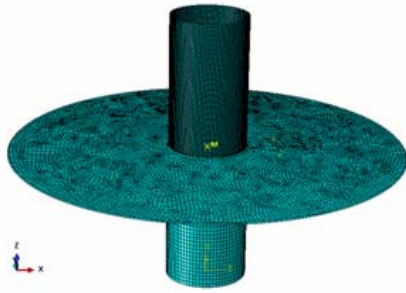


Figure-24(a). Finite element mesh.



(b) Axisymmetric FEM model for stretch flanging (Dewang Y. *et al*, 2014).

Location of prediction of failure along die profile radius was investigated after doing finite element simulation of non-axisymmetric stretch flanging process using FE software package ABAQUS. They utilized C3D8R solid elements for meshing for sheet metal blank (Dewang Y. *et al.*, 2014).

5. PARAMETRIC STUDY

5.1. Effect of geometrical parameters

There are various geometrical parameters in stretch flanging process such as initial flange length, flange length to flange radius, final flange height and curvature radius of punch and trim radius of blank which greatly influence the formability of the process. Figure-25 shows the various portions of stretch flange. Initial flange length is one of the important parameter of stretch flanging process. Initial flange length is the portion of the sheet metal before flanging to bend it along the die profile. It was observed that circumferential strain along free edge decreases with decrease in initial flange length as shown in Figures 26, 27 and 28, respectively (Wang C.T. *et al*, 1995; Li. D. *et al*, 2007; Dewang Y. *et al*, 2014).

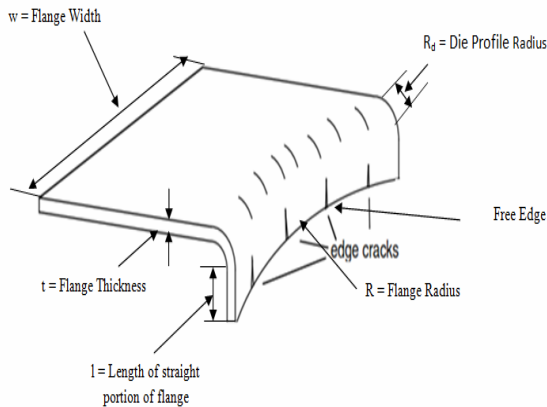


Figure-25. Definition of various portions of stretch flange (Dewang Y. *et al*, 2014).

In case of stretch flanging of “V” shaped metal blanks, the maximum free edge strain with 6.4 mm initial flange length decreases to 18% in comparison with that of

19.6 mm as per Figure-26 (Li D. *et al*, 2007). It was also found that maximum circumferential strain at flange edge increases with increase in initial flange length as shown in Figure-29 (Wang C.T. *et al*, 1995).

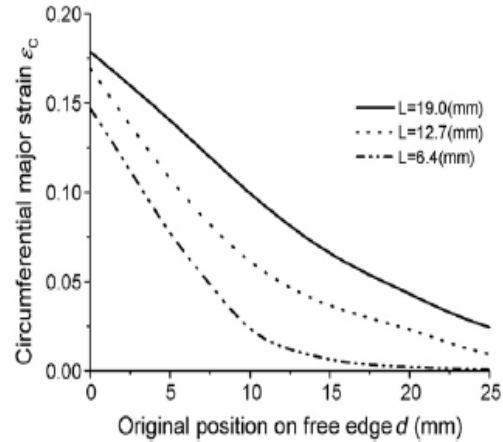


Figure-26. Effect of initial flange length on circumferential strain distribution (Li D. *et al*, 2007).

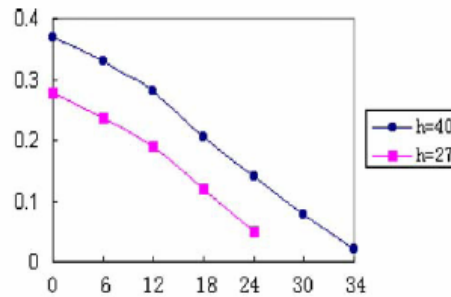


Figure-27. Effect of initial flange length on circumferential strain distribution (Feng X. *et al*, 2007).

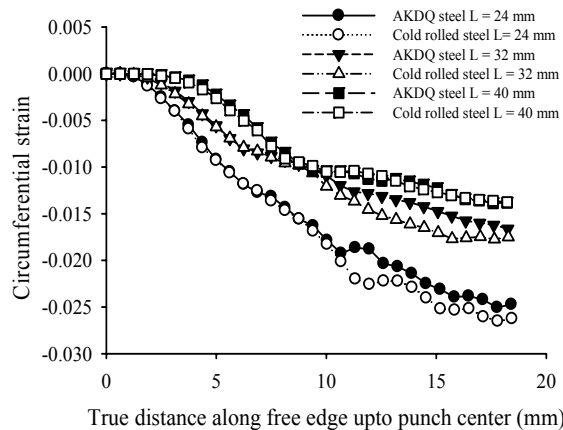


Figure-28. Effect of initial flange length on circumferential strain distribution (Dewang Y. *et al*, 2014).

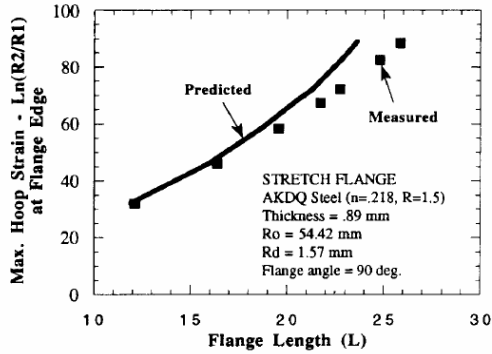


Figure-29. Effect of flange length on maximum circumferential strain (Wang C.T. *et al*, 1995).

Length of straight side (L) and radius of curved range (R) are the two main geometrical parameters in stretch flanging process which greatly influence the tension leading to crack at the flange edge. In past researchers studied the effect of these two parameters in a combined manner and designated this as the ratio of length of straight side and radius of curved range as (L/R) ratio. It is found that circumferential strain increases with increases in (L/R₀) ratios as shown in Figure-30 and Figure-31 (Wang N.M. *et al*, 1984; Feng X. *et al*, 2004). It was also observed that for large (L/R₀) ratios that the maximum strain in stretch flanging of “V”-shaped sheet metal blanks, which tends to converge to a limiting value as shown in Figure-32 (Wang N.M. *et al*, 1984).

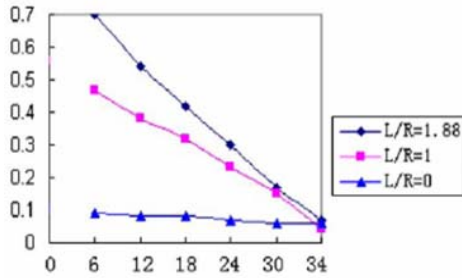


Figure-30. Effect of (L/R₀) ratios on circumferential strain (Feng X. *et al*, 2004).

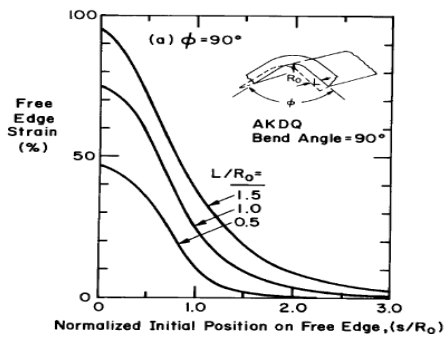


Figure-31. Effect of (L/R₀) ratios on free edge strain (Wang N.M. *et al*, 1984).

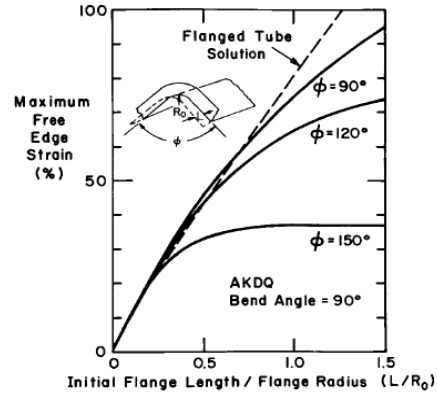


Figure-32. Effect of (L/R₀) ratios on maximum free edge strain (Wang N.M. *et al*, 1984).

Flange angle is another vital parameter of stretch flanging process. Flange angle is the angle subtended by the sheet metal portion after flanging w.r.t. to the unbent or straight portion of the flange as shown in Figure-25. It is also recognized as the included angle between the two surfaces of the flange after flanging operation. In flanging, generally the flange angle varies from 90 degree and it can be formed to obtain various other flange angles such as 45, 120, 135, 140, 160 degrees as per requirements. It was found that in stretch flanging of “V” shaped blanks, circumferential strain decreases with increase in flange angle (the included angle of “V”) as shown in Figure-33 (Wang N.M. *et al*, 1984; Li D. *et al*, 2007). It was observed from Figure-33 that when flange angle was 120 degree, then the maximum free edge strain is 5.9 times that of 160 degree flange angle (Li D. *et al*, 2007). Figure-34 shows that maximum free edge strain distribution decreases with increase in flange angle (Wang N.M. *et al*, 1984). On the other hand it was also found that circumferential strain along free edge decreases with decrease in flange angle for stretch flanging of AKDQ steel as shown in Figure-35 (Wang C.T. *et al*, 1995).

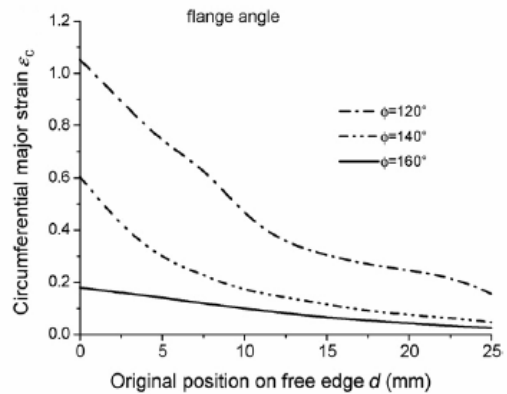


Figure-33. Effect of flange angle on circumferential strain distribution (Li D. *et al*, 2007).

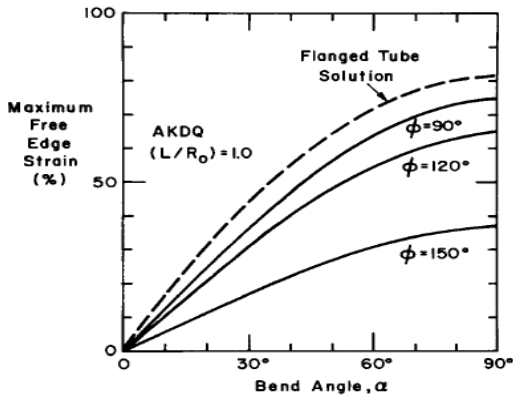


Figure-34. Effect of flange angle on maximum free edge strain (Wang N.M. *et al*, 1984).

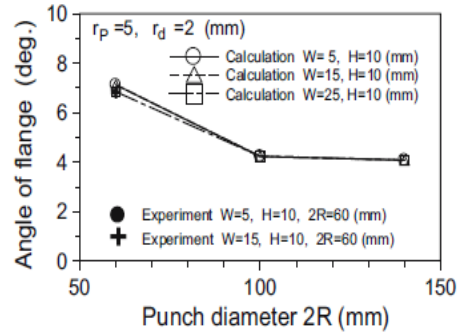


Figure-37. Effect of web-width on flange angle (Huang Y.M., 2007).

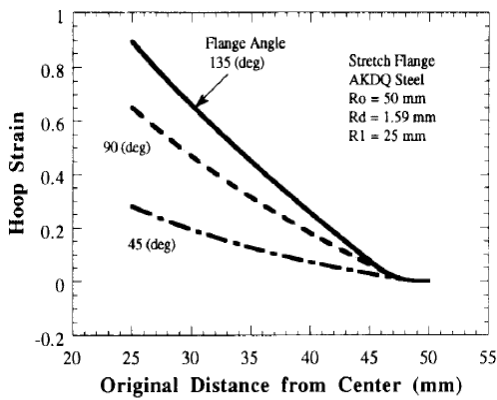


Figure-35. Effect of flange angle on hoop strain (Wang C.T. *et al*, 1995).

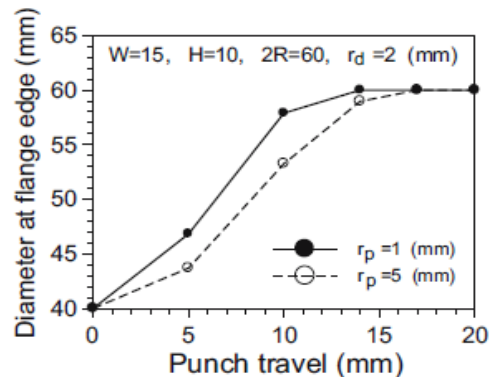


Figure-38. Effect of punch corner radius on diameter at flange edge (Huang Y.M., 2007).

Curvature radius of punch or profile radius of punch is another geometrical parameter which influences the stretch flanging process. It was observed that circumferential strain decreases with increase in curvature radius of punch as shown in Figure-36 (Feng X. *et al*, 2004). Some parametric studies were also carried out on stretch flanging process, which shows that web width has no influence on flange angle as shown in Figure-37, while the tendency of flange thinning decreases with increase in punch diameter as per Figure-38 (Huang Y.M., 2007).

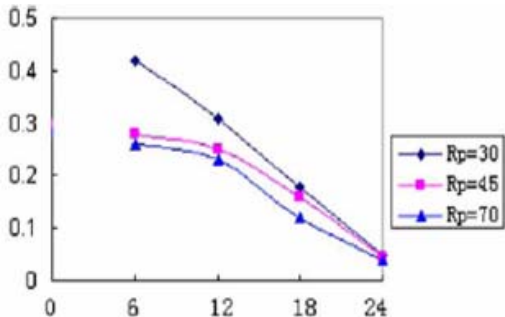


Figure-36. Effect of curvature radius of punch on strain (Feng X. *et al*, 2004).

In another parametric analysis of stretch flanging process it was found that final flange height decreases with increase in trim radius, while circumferential and radial strain increases with increase in prestretching as shown in Figure-39 and Figure-40, respectively.

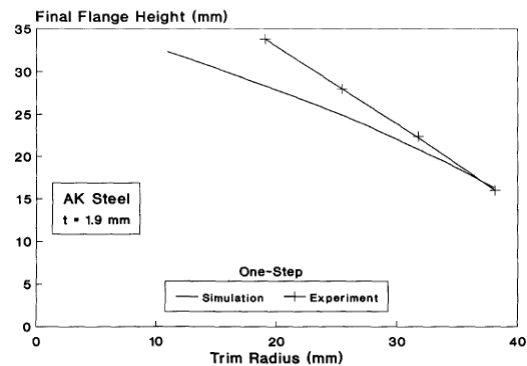


Figure-39. Effect of trim radius on final shape height (Demeri M.Y., Tang S.C., 1991).

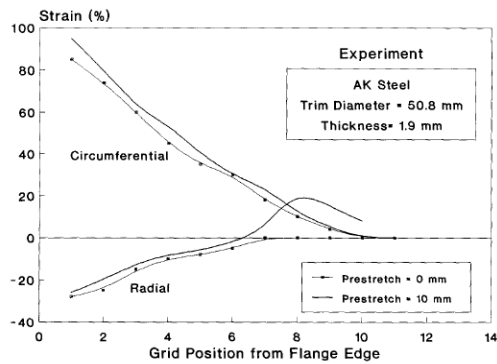


Figure-40. Effect of prestretching on strain distribution in flange (Demeri M.Y. and Tang S.C., 1991).

5.2. Effect of material parameters

Again there are parameters related to the materials in the area of sheet metal forming processes, which plays a major role in affecting the formability of the process. In the area of sheet metal stretch flanging process there were material parameters such as strain hardening exponent, normal anisotropy parameter or plastic strain ratio which affected the feasibility of the process. Strain hardening exponent is an important parameter in sheet metal forming. It is denoted as n and is a materials constant (material property) which is used in calculating stress-strain behavior. It signifies the strain hardening or work hardening characteristics of material i.e., the higher the value of n , the higher is the rate at which the material work hardens. A material with the value of n is predefined for cold working; because it results in superior mechanical properties. Another reason for its significance is that it is an indicator of the stretch formability of a material. It is so because n equal the true strain at the ultimate point which is the limiting value of strain for uniform deformation. In the formula as given in equation (12) which is commonly known as power law

$$\sigma = K \cdot \epsilon^n \quad (12)$$

Where

σ = applied stress

ϵ = strain

K = strength coefficient

In view of the effect of strain-hardening exponent upon the formability of stretch flanging process, some parametric studies were carried out. It is observed that circumferential strain along free edge decreases with increase in strain hardening exponent (Wang, N.M. *et al*, 1984; Li D. *et al*, 2007). Figure- 41 shows the effect of circumferential major strain along free edge and it was observed that the variation of free edge strain is opposite to the variation in strain hardening exponent, and free edge strain was maximum for least strain hardening exponent of 0.26 (Li D. *et al*, 2007). Besides this it was also observed from Figure-42 that due to the effect of strain hardening exponent, the maximum free edge strain is relatively smaller.

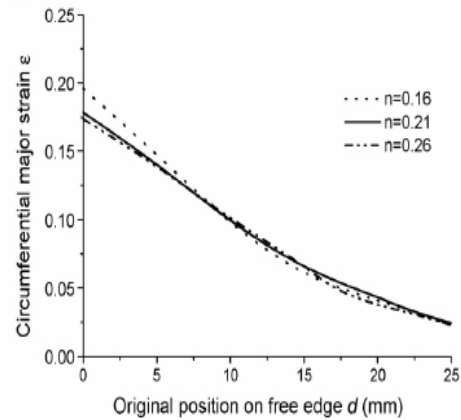


Figure-41. Effect of strain hardening exponent on circumferential strain (Wang N.M. *et al*, 1984).

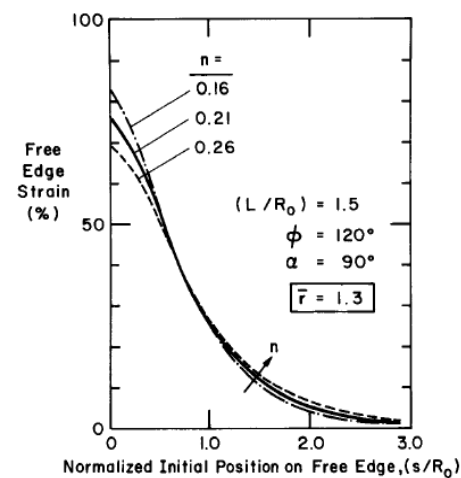


Figure-42. Effect of strain hardening exponent on free edge strain (Wang N.M. *et al*, 1984).

The r value, or plastic strain ratio, relates to drawability and is also known as the anisotropy factor. This is defined as the ratio of the true width strain to the true thickness strain in the uniform elongation region of a tensile test as per equation (13).

$$r = \frac{\epsilon_w}{\epsilon_t} = \frac{\ln\left(\frac{w}{w_0}\right)}{\ln\left(\frac{t}{t_0}\right)} \quad (13)$$

The r value is a measure of the ability of a material to resist thinning. In drawing, material in the flange is stretched in one direction (radially) and compressed in the perpendicular direction (circumferentially). A high r value indicates a material with good drawing properties. In analysis of sheet metal stretch flanging process; it was observed that circumferential strain along free edge decreases with



increase in normal anisotropy parameter (r) as shown in Figure-43 and Figure-44 (Li D. *et al*, 2007; Wang N.M. *et al*, 1984).

In analysis of stretch flanging of aluminum alloys by fluid forming fracture limit was determined by plastic strain ratio, strain hardening exponent, uniform strain. It was found that higher the limit of these material parameters higher will be the fracture limit (Asnafi N., 1999).

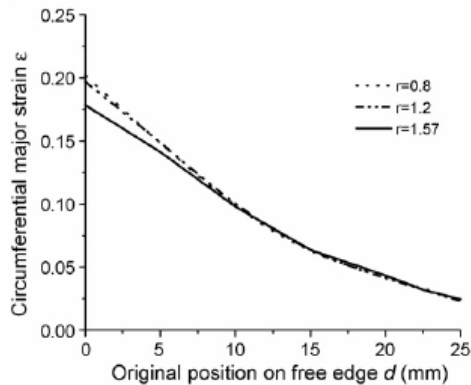


Figure-43. Effect of normal anisotropy parameter on circumferential strain (Li D. *et al*, 2007).

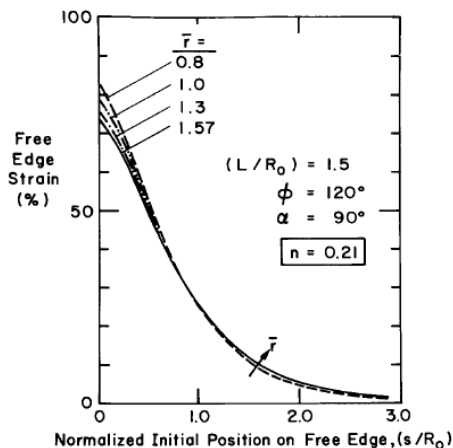


Figure-44. Effect of normal anisotropy parameter on free edge strain (Wang N.M. *et al*, 1984).

6. CONCLUSIONS

With the growth and development of computational facilities, it has certainly pushed the usage of finite element method for finite element simulation of stretch flanging process. In past three decades, in the domain of finite element analysis a lot of improvement was made by previous researchers i.e., from FEM based computer program to highly improved and computationally efficient FEM commercial packages and coding facilities. From the review, it can be seen that various parametric studies were also carried out which had greatly improved the stretch flanging process. It is found

from FEM based parametric studies that geometrical parameters have greater influence on formability of stretch flange in comparison to material parameters. In view of usage of materials used for FEM simulation of stretch flanging process, the trend is now shifted towards aluminum alloys for manufacturing of stretch flanges which is towards ferrous alloys in past. It has been observed that usage of aluminum alloys will impart advantages of light weight products with higher strength and also higher corrosion resistance for making of stretch flanges especially in automobile industry. It is also concluded from review, that dynamic explicit approach is widely employed for finite element analysis of stretch flanging process. Hence, finite element method is a very important, accurate and vital tool for better and efficient design of stretch flanging process.

Future work in the domain of finite element analysis of stretch flanging process may include the more concentrated efforts on the failure prediction using continuum damage mechanics and also by considering different formability based failure criteria for obtaining defects free products and to ascertain and to redefine the forming limits of stretch flanging process. In view of parametric studies based on FEM the effect of parameters such as blank-holding force, punch-die clearance and heat treatment (annealing temperature) can also be considered for clearer and better understanding of stretch flanging process.

REFERENCES

- Asnafi N. 1999. On stretch and shrink flanging of sheet aluminium by fluid forming. *Journal of Materials Processing Technology*. 96: 198-214.
- Bao Y.D. and Huh H. 2007. Optimum design of trimming line by one-step analysis for auto body parts. *Journal of Materials Processing Technology*. 187-188: 108-112.
- Brunet M. 1996. The prediction of necking and failure in 3D sheet forming analysis using damage Variable. *Journal De Physique*. III: 6.
- Butcher C., Chen Z. and Worswick W. 2006. A lower bound damage-based finite element simulation of stretch flange forming of al-mg alloys. *International Journal of Fracture*. 142: 289-298.
- Chen Z., Worswick M.J., Pilkey A.K. and Lloyd D.J. 2005. Damage percolation during stretch flange forming of aluminum alloy sheet. *Journal of the Mechanics and Physics of Solids*. 53:2692-2717.
- Dewang Y., Hora M.S. and Panthi S.K. 2014. Analysis of stretch flanging process using FEM to study deformation behavior of flange. *International Conference on Emerging Materials and Processes*. pp: 247-252.



- Dewang Y., Hora M.S. and Panthi S.K. 2014. Finite element analysis of non-axisymmetric stretch flanging process for prediction of location of failure. *Procedia Materials Science*.5: 2054-2062.
- Dudra S. and Shah S. 1998. Stretch flanges: Formability and trimline development. *Journal of Materials Shaping Technology*. 6(2): 91-101.
- Feng X., Zhongqin L., Shuhui L. and Weili X. 2004. Study on the influences of geometrical parameters on the formability of stretch curved flanging by numerical simulation. *Journal of Materials Processing Technology*. 145: 93-98.
- Hu P., Li D.Y. and Li Y.X. 2003. Analytical models of stretch and shrink flanging. *International Journal of Machine Tools and Manufacture*. 43: 1367-1373.
- Hu W. and Wang Z.R. 2002. Anisotropic characteristics of materials and basic selecting rules with different sheet metal forming processes. *Journal of Materials Processing Technology*. 127: 374-381.
- Huang Y.M. 2007. An elasto-plastic finite element analysis of the sheet metal stretch flanging process. *Int. J Adv Manuf Technol*. 4: 3641-3648.
- Huang Y.M. 2007. Finite Element Analysis of the sheet metal stretch flanging process. The ninth international conference on automation technology, Taiwan.
- Kacem A., Krichen A. and Manach P.Y. 2011. Occurrence and effect of ironing in the hole-flanging process. *Journal of Materials Processing Technology*. 211: 1606-1613.
- Krichen A., Kacem A. and Hbaieb M. 2011. Blank-holding effect on the hole-flanging process of sheet aluminum sheet. *Journal of material processing technology*. 211: 619-626.
- Li D., Luo Y., Peng Y. and Hu P. 2007. The numerical and analytical study on stretch flanging of V-shaped sheet metal. *Journal of Materials Processing Technology*. 189: 262-267.
- Nielsen C.V., Zhang W., Alves L.M. and Martins P. 2013. Modeling of thermo-electro-Mechanical Manufacturing Processes: Applications in Metal Forming and Resistance Welding. 7: 120.
- Semiatin S.L. 2006. *Metalworking: Sheet Forming*. ASM Handbook. Vol. 14B.
- Simha C.H.M., Grantab R. and Worswick M.J. 2008. Application of an extended stress-based forming limit curve to predict necking in stretch flange forming. *Journal of Manufacturing Science and Engineering*. 130: 051007-1-051007-11.
- Vafaeseefat A. and Khanahmadlu M. 2011. Comparison of the numerical and experimental results of the sheet metal flange forming based on shell-elements types. *International Journal of Precision Engineering and Manufacturing*. 12(5): 857-863.
- Wang C.T., Kinzel G. and Altan T. 1995. Failure and wrinkling criteria and mathematical modeling of shrink and stretch flanging operation in sheet metal forming. *Journal of Materials Processing Technology*. 53: 759-780.
- Wang N.M., Johnson L.K. and Tang S.C. 1984. Stretch flanging of V shaped sheet metal blanks. *Applied Metal working*. 3(3): 281-291.
- Worswick M.J. and Finn M.J. 2000. The numerical simulation of stretch flange forming. *International Journal of Plasticity*. 16: 701-720.
- Yeh F.H., Wu M.T. and Li C.L. 2007. Accurate optimization of blank design in stretch flange based on a forward-inverse prediction scheme. *International Journal of Machine Tools and Manufacture*. 47: 1854-1863.
- Yingwei C. L. L. and Shanliang L. 2010. Finite element simulation and control method on springback of stretch flanging in rubber forming. *International Conference on Digital Manufacturing and Automation, IEEE*. pp. 734-737.